

Quasars as Cosmological Probes: The Ionizing Continuum, Gas Metallicity and the W_λ -L Relation

Kirk Korista,

Department of Physics, Western Michigan University, Kalamazoo, MI 49008

Jack Baldwin¹

Cerro Tololo Interamerican Observatory, National Optical Astronomy Observatories, Tucson, AZ 85726

and

Gary Ferland

Department of Physics and Astronomy, University of Kentucky, Lexington, KY 40506

ABSTRACT

Using a realistic model for line emission from the broad emission line regions of quasars, we are able to reproduce the previously observed correlations of emission-line ratios with the shape of the spectral energy distribution (SED). In agreement with previous studies, we find that the primary driving force behind the Baldwin Effect ($W_\lambda \propto L^\beta$, $\beta < 0$) is a global change in the SED with quasar luminosity, in that more luminous quasars must have characteristically softer ionizing continua. This is completely consistent with observations that show (1) a correlation between L_{uv} and α_{ox} and α_{uvx} , (2) correlations of SED shape sensitive line ratios with α_{ox} , α_{uvx} , and L_{uv} , and (3) correlations between line equivalent widths and α_{ox} , α_{uvx} , and L_{uv} . However, to explain the complete lack of a correlation in the $W_\lambda(\text{N v}) - L_{uv}$ diagram we propose that the more luminous quasars have characteristically larger gas metallicities (Z). As a secondary element, nitrogen's rapidly increasing abundance with increasing Z compensates for the losses in $W_\lambda(\text{N v})$ emitted by gas illuminated by softer continua in higher luminosity quasars. A characteristic relationship between Z and L has an impact on the $W_\lambda - L_{uv}$ relations for other lines as well. For a *fixed* SED, an increasing gas metallicity reduces the W_λ of the stronger metal lines (the gas cools) and that of Ly α and especially He II (because of the increasing metal opacity), while the weaker lines (e.g., C III] 1909) generally respond positively. The interplay between the effects of a changing SED and Z with L results in the observed luminosity dependent spectral variations. All of the resulting dependences on L_{uv} are within the range of the observed slopes.

Subject headings: galaxies: quasars: emission lines — cosmology: large-scale structure of universe

¹CTIO is operated by AURA, Inc. under contract to the National Science Foundation.

1. Introduction

Since their discovery as the most distant and luminous discrete objects in the Universe, it has been hoped that somehow quasars could be used as “cosmological candles” to measure the expansion parameters (q_0 and H_0) of the universe. With the discovery of the Baldwin Effect (Baldwin 1977), whereby the emission line equivalent widths scale inversely with the quasar luminosity, that hope is half-realized. Unfortunately, the very large scatter in these correlations (Baldwin, Wampler & Gaskell 1989; Kinney, Rivolo & Koratkar 1990; Osmer, Porter & Green 1994) have curtailed their usefulness. What remains is to understand the mechanism of the formation of quasar emission lines well enough so that this scatter can somehow be calibrated in terms of observable parameters, and then removed.

A second major goal of studies of distant quasars is to use them as probes of the first generations of nucleosynthesis in the young Universe. There is evidence of wide variations in the atomic abundances in the BLRs of different quasars, and that the spectroscopic effects of this can be measured out to very large redshifts (Hamann & Ferland 1992; Hamann & Ferland 1993: HF93; Ferland et al 1996). Again, full interpretation requires a proper understanding of the formation of quasar emission lines.

There is mounting evidence that the line strengths strongly depend on the spectral energy distribution (SED) in the UV – X-Ray range. (Netzer, Laor, and Gondhalekar 1992, Zheng et al. 1995, Green 1996, Wang et al. 1998). In addition, many studies have found a correlation between α_{ox} and luminosity (cf. Zamorani et al. 1981; Wilkes et al. 1994; but see also LaFranca et al 1995 and Avni et al 1995 for discussion of conflicting results). This link through α_{ox} offers a promising explanation of the observed W_λ – L_{uv} relations (Wang et al 1998; Green 1998). Here we investigate to what extent we can reproduce these observed effects using realistic photoionization models of the BLR, and study the degree to which the additional parameter of metallicity must also be taken into account.

2. LOC Models

We describe the BLR in terms of the “Locally Optimally-emitting Clouds” (LOC) model, discussed in Baldwin et al. (1995). This model assumes that the many individual gas clouds which make up the

BLR have a wide range of internal densities and sizes and occur over a wide range in distance from the central continuum source. Under these conditions the emitted spectrum is controlled by powerful selection effects introduced by the atomic physics and basic radiative transfer effects (see also Korista et al. 1997), and the typical observed quasar spectrum is naturally produced.

This picture is supported by the line-continuum reverberation studies, showing that gas having a range of densities must exist over a wide range of radii. (Ferland et al. 1992; Peterson 1993). The spectrum predicted by the LOC depends on global integrations, over gas density at a particular location, and over radius. Results depend weakly on the density distribution near those distributions that produce typical quasar spectra, and only somewhat on the radial distribution. This can be contrasted to single cloud models, which often are described by an ionization parameter (Davidson & Netzer 1979) and whose predicted spectrum has a powerful dependence on this parameter. The LOC models fit the observed spectrum better with fewer free parameters than do single cloud models. But more importantly, the LOC approach is a more physical model because unless the BLR clouds have a remarkably restricted range of properties, we will in fact observe the optimally emitting clouds for most lines. The emission line spectrum from clouds distributed in gas density and radius is much less sensitive to changes in the gas abundances and SED than is that emitted by a single cloud of a fixed gas density and ionization parameter. Thus analyses that use a single cloud to investigate the expected spectral variations with changes in gas abundances or SED may derive misleading results.

We have generated extensive grids of photoionization models similar to those shown in Korista et al. (1997), and integrated over the cloud properties to obtain predicted LOC spectra. We did this for a wide range of SED and metallicities, with the goal of finding the dependence of the final LOC spectra on these two parameters. To the extent that the geometry is independent of luminosity, this comparison will not be affected at all by the assumed cloud distributions, for which we have just used the standard LOC parameters: $f(r) \propto r^{-1}$, an outer radius corresponding to a hydrogen ionizing photon flux of $10^{18} \text{ s}^{-1} \text{ cm}^{-2}$, and $g(n_H) \propto n^{-1}$, integrated from $\log n_H = 8$ to $\log n_H = 12 \text{ cm}^{-3}$ (see Baldwin et al. 1995 for definitions of $f(r)$ and $g(n_H)$). For simplicity we took

the ionizing continuum shape to be a single power law, $f_\nu \propto \nu^\alpha$, and varied the spectral index over the range $-2 < \alpha < -1$, normalizing each SED to have the same number of photons/s below 912 Å. Our prescription for abundances is given in Table 1, where “metals” refers to all elements except H, He and N. These variations with increasing Z (= metals/H relative to the solar abundance ratio) are similar to the HF93 galactic chemical enrichment models whose major feature is that nitrogen is built up as a delayed secondary element, at a rate $N/H = b(Z)Z^2$, with $b(Z) < 1$. Here we have chosen $b(Z) = b = 0.5$, consistent with the rapid star formation enrichment models presented in HF93. This particular choice of $b(Z)$ does not affect the structure of the cloud or the strengths of any non-nitrogen lines in any significant manner. The helium abundance is scaled gently with Z as in HF93, however, for simplicity we have chosen to scale all metals (excluding N) with Z from solar abundances.

Figure 1 shows the results for some of the stronger UV lines. The upper panels show predicted equivalent widths as a function of α and Z , while the bottom panels show corresponding intensity ratios. As stressed by HF93, the strength of N V $\lambda 1240$ relative to either C IV $\lambda 1549$ or He II $\lambda 1640$ is a good metallicity indicator, as can be seen in the lower-left panel. The lower-right panel shows these same ratios for $Z = 1$ and various continuum shapes. The N V/He II and N V/C IV line ratios have little dependence on α . Although the N V/He II ratio does become sensitive to the continuum shape if a UV bump is introduced (factor of ≈ 2 variation; see also Ferland et al. 1996), these variations are relatively small compared to the order of magnitude range of observed ratios. The N V/C IV ratio is virtually independent (± 0.05 dex) of any reasonable quasar continuum. Conversely, the ratios Ly α /C IV and Ly α /O VI $\lambda 1034$ are not affected much at all by changes in the metallicity but depend strongly on the continuum shape, showing the steepest dependence on α of any of the ratios of strong lines which we examined.

There are several reasons for these dependencies. The O VI and C IV lines have ionization potentials much higher than hydrogen. The abundance of these ions relative to hydrogen is sensitive to the form of the continuum between 13.6 eV and 100 eV. This was the basis of the earlier investigations by Zheng et al. (1995), Green (1996) and others. The intensities of these lines depend only weakly on the metallicity be-

cause of the strong thermostat effect introduced by such strong cooling lines. As the abundance of C or O goes up the gas cools more effectively and so the temperature falls as the stronger lines maintain or even diminish in their intensities. Nitrogen lines do introduce a strong metallicity dependence since N is initially a rare element, and its abundance relative to hydrogen goes up as the square of the overall metallicity. This large increase in abundance does allow the N V to grow stronger as it takes on more of the cooling. The equivalent width of He II $\lambda 1640$ diminishes with increasing Z as the metals become increasingly important sources of opacity. To a lesser degree this is also true of Ly α $\lambda 1216$.

Ferland et al. (1992) and Shields, Ferland, & Peterson (1995) pointed out that Ly α may be significantly contaminated with other emission (including C III $\lambda 1176$, S III $\lambda 1190$, S V] $\lambda 1198$, Si III $\lambda 1207$, and especially He II $\lambda 1216$ and O V] $\lambda 1218$). However, the model predictions find that these are contaminants at the level of 8% – 15% the intensity of Ly α over the full range in SED and Z shown in Figure 1. Our models predict a similar level of contamination to O VI $\lambda 1034$ due to Ly β $\lambda 1025$. Neither set of contaminants is important to the results presented here.

In addition to the results shown in Figure 1, we also examined the behavior of the equivalent widths of the $\lambda 1400$ (sum of Si IV $\lambda 1397$, O IV] $\lambda 1402$, S IV] $\lambda 1405$) and $\lambda 1900$ (sum of C III] $\lambda 1909$, Si III] $\lambda 1892$, Al III $\lambda 1860$) blends and of Mg II $\lambda 2800$, and of all intensity ratios between the different lines. Note that the predicted strength of the $\lambda 1900$ blend does not include emission from Fe III UV 34, a major contributor to this blend in some quasars (Baldwin et al. 1996; Laor et al. 1997). The four intensity ratios shown in Figures 1c and 1d were chosen because they had the strongest dependence on either α or Z , and therefore will give the best leverage for measuring these underlying parameters.

3. Comparison with Observations

It is possible to directly test the model results with respect to α . The work of Zheng et al (1995) and Wang et al (1998) shows that the intensity ratios O VI/Ly α and C IV/Ly α directly correlate with an observed indicator of the shape of the ionizing continuum, α_{ox} . Wang et al. show that their C IV/Ly α data set can be fitted by single-cloud models, provided they choose the correct ionization parameter and gas

density. Figure 2 shows that the results from the LOC simulations, with $Z = 1$, also generally reproduce the observed trends in these intensity ratios, but without requiring adjustable parameters.

Many studies have now confirmed the existence of W_λ - L_{uv} correlations for most of the strong emission lines in quasar spectra. These results are summarized in columns 4 and 6 of Table 2, which list the observed slopes and intercepts of these correlations, taken from the references cited in column 7. These observed relationships are such that the strongest effect is seen in O VI followed by C IV, He II, and then Ly α . Figure 1b shows that the same sequence results from the LOC models, on the assumption that α increases (spectrum becomes softer) with increasing luminosity. This lends credence to the idea that the Baldwin Effect is at least in part due to a systematic change in the incident continuum shape with luminosity.

However, there is a glaring discrepancy between the predicted trends in Figures 1b and 1d and the observed behavior of the N V λ 1240 line. The LOC models (and for that matter any single-cloud model) predict that W_λ (N V) should vary as strongly with α (and therefore with luminosity) as does W_λ (C IV), whereas the observations show almost no correlation with L_{uv} . Equivalently, N V/C IV should be nearly independent of L_{uv} , but the work of HF93 shows that higher values of N V/C IV are systematically found at higher redshifts and/or higher L . Figure 6 of Osmer et al. (1994) clearly shows the near absence of an W_λ (N V)- L_{uv} relation, and the correspondingly strong dependence of N V/C IV on luminosity, for high-redshift quasars. This must mean that continuum shape is not the only parameter.

4. Metallicity as a second parameter

Figures 1a, 1b suggest the following solution: while most lines' W_λ diminish with increasing luminosity due to a systematic softening of the SED, a systematic increase in the gas metallicity Z (and $N/H \propto Z^2$) with quasar luminosity could, in the case of N V, compensate for this loss and result in an W_λ that is roughly constant with the quasar luminosity. Note that W_λ (N V) decreases by roughly 0.8 dex over the range of $1.2 < \alpha < 1.8$, while it increases by virtually the same amount over the range of $1 < Z < 10$. The range in α was chosen to represent the observed range for quasars (Zamorani et al. 1981; Wilkes et al. 1994). The range in Z is within the range which might be

at least reasonable according to population synthesis models (HF93), and a detailed study by Ferland et al (1996) shows that in some quasars Z must be greater than at least 5. Thus for the observed range of SEDs, there is a reasonable range in $N/H \propto Z^2$ that can offset the expected change in W_λ (N V), provided that both SED and Z depend on L .

The models do not tell us how to map α into L . For the present study, we simply adopt the empirical $\alpha_{ox} - L$ relation found by Wilkes et al. (1994); thus we adopt their choice of $H_o = 50 \text{ km s}^{-1} \text{ Mpc}^{-1}$ and $q_o = 0$. This gives the effective 2500 Å to 2 keV continuum slope (α_{ox}); we made a slight adjustment in its logarithmic zero point to reference the continuum luminosity at 1550 Å. Since the line equivalent widths and continuum-shape sensitive line ratios are observed to correlate with α_{ox} , the latter must be strongly correlated with the true measure of the ionizing continuum's hardness. Wang et al. (1998) defined an α_{uvx} , a measure of the ratio of fluxes at 1350 Å and 1 keV, closer to the ionizing photons, and reaffirmed this assertion in a large sample of quasars.

As an initial guess at the $L - Z$ relation, we assumed a metallicity $Z \approx 1$ for the lowest luminosity sources and $Z \approx 10$ for the highest. This is consistent with the slopes of the N V/C IV and N V/He II dependences on L_{uv} given by HF93 (their Fig. 7), when mapped back to metallicity Z using our Fig 1a. Since L and α_{ox} are also correlated, we simply assigned $Z = 1$ to $\alpha_{ox} = 1.2$, $Z = 10$ to $\alpha_{ox} = 1.8$, and a power law in α_{ox} and Z in between. Then using the relationship between $L_\nu(1550)$ and α_{ox} , this example results in the simple power law relation $\log Z = 0.183 \log(L_\nu(1550)/10^{30}) + 0.477$. The range in α_{ox} and Z results in a range in $L_\nu(1550)$ of $10^{27.40}$ to $10^{32.85} \text{ ergs s}^{-1} \text{ Hz}^{-1}$.

In the spectral simulations, we assumed a simple power law continuum SED and so α_{ox} is identical to α : 1.2, 1.4, 1.6, 1.8. In accordance with the above expression each power law SED was then assigned to its respective metallicity Z : 1, 2, 5, 10. Four separate grids of cloud emission were then computed and integrated, as described above. The resulting predicted emission line/continuum relations and their observed counterparts are given in Table 2. In each case the predicted relationships were fitted with a straight line, usually a good approximation. The slopes β and intercepts c are listed in the table, where the fit is to $y = c + \beta x$. In four cases, a significant break in the slope of the predicted relation forced a double-

power law fit, and both relations are given. The simulated W_λ for each emission line is referenced to the continuum at 1215 Å and a global covering fraction of 0.5 is assumed. These affect only the intercepts, not the slopes. Finally, we point out that relationships involving $L_\nu(1550)$ in Table 2 are not strictly comparable, since different investigators (column 7) assumed different values of the deceleration parameter q_o (all assumed $H_o = 50 \text{ km s}^{-1} \text{ Mpc}^{-1}$). When known, the assumed values of q_o are listed in the footnotes of Table 2. The effect of different choices of q_o is non-uniform in the W_λ - L_{uv} plane, and its effect on the W_λ - L_{uv} slope can be comparable to the typically quoted uncertainty in the slope's measurement of ± 0.04 .

Given the simplicity of our assumptions, the predicted relationships match the observed ones surprisingly well. The general lack of a W_λ - L_{uv} relationship in N V and the trends in the different slopes for different lines are reproduced. We note that while the overall behavior of the N V/He II vs. N V/C IV relationship is matched very well by our models, we do not reproduce the highest observed values. The primary reason for this is that our models do not predict a large enough $W_\lambda(\text{N V})$ at a given L_{uv} . Of the lines studied here, this line will be by far the most sensitive to the choice of abundances (see Figure 1b). Under our hypothesis, our simulations also predict that the line ratios $\text{Ly}\alpha/\text{C IV}$ and $\lambda 1900/\text{C IV}$ should increase with increasing L_{uv} , as is observed (Osmer et al. 1994). This is simply a result of differing slopes of their respective W_λ - L_{uv} relations. Many investigators have suggested this change in the spectrum to be due to a shift in ionization parameter to lower values at larger L_{uv} (e.g., Mushotzky & Ferland 1984). However, we would argue that this change in the line spectrum is due to a characteristic shift to softer incident continua and higher Z with increasing L_{uv} . Of these two effects, the metallicity has the largest impact on the $\lambda 1900/\text{C IV}$ ratio. Observationally, the challenge will be to tighten these and other key global relationships. Table 2 shows that these stronger lines of quasars do carry sufficient information to constrain the proposed evolution of the SED and Z with L .

5. Summary and Discussion

We have shown here that including a Z - L effect in addition to a SED- L relation allows us to simultaneously reproduce the observed correlations with L

of the equivalent widths and intensity ratios of all of the strong UV lines, particularly N V. As a secondary element, nitrogen's rapidly increasing abundance with increasing Z compensates for the losses in $W_\lambda(\text{N V})$ emitted by gas illuminated by softer continua in higher luminosity quasars. For a *fixed* SED, an increasing gas metallicity reduces the W_λ of the stronger lines of other heavy elements (the gas cools) and that of Ly α and especially He II (because of the increasing metal opacity), while the weaker metal lines (e.g., intercombination lines such as C III] 1909) generally respond positively. Weak lines such as O IV] $\lambda 1402$, formed in the He $^{++}$ zone, suffer from the significant drop in temperature and their intensities remain roughly constant with increasing Z . The interplay between the effects of a changing SED and Z with L results in the observed luminosity dependent spectral variations.

However, the photoionization models only predict relations with α and Z . To get to relations with L we have had to adopt both an α - L relation, and a Z - L relation. These two relations or at least their combined effect must still be calibrated empirically, from comparing emission line parameters to continuum fluxes, before the Baldwin Effect can be used as a real luminosity indicator for cosmological tests.

Why should we expect a global relationship between Z and quasar luminosity? HF93 and Ferland et al. (1996) showed that the average N V/C IV and N V/He II ratios increase systematically with redshift and/or luminosity. They attributed this change in line ratios to an increase in metallicity, as we do here. HF93 proposed that the luminosity dependence of metallicity is really a mass-metallicity relation. Because of their deeper potential wells, higher-mass galaxies are better able to retain gas deposited during stellar evolution than are lower-mass galaxies, so they have a more rapid buildup of heavy elements in their nuclear regions. Coupling this scenario with observations showing that the most luminous quasars tend to reside in the most massive galaxies (McLeod & Rieke 1995a, 1995b; Bahcall et al. 1997) leads to a natural explanation for a global relationship between quasar luminosity and gas metallicity. To the extent that luminosity evolution affects individual quasars, the redshift-metallicity dependence would also require a steady decrease in metallicity with time in individual objects. HF93 suggested that this was due to dilution by lower- Z gas falling into the nuclear regions throughout the lives of these galaxies.

In addition, the simplest accretion disk models predict that more luminous quasars should in general emit softer continua (Netzer et al. 1992), though the continuum emission mechanism is far from understood. Together, these form the basis of the proposed global L -SED- Z relationship.

Can the noise in the Baldwin Effect be eliminated, much as an observer corrects for reddening? Metallicity should scale with the mass of the host galaxy and not necessarily the quasar luminosity, thus introducing noise. The importance of this effect can be estimated from Figure 3, which compares the observations of Osmer et al. (1994) to the range covered by our models on the $W_\lambda(\text{C IV})$ - L diagram as metallicity is varied from half solar to ten times solar. Just making a correction on the basis of the N V/C IV ratio may remove much of the scatter at high redshifts; this is something that can be tested empirically. There are likely to be additional sources of scatter as well: a spread in α at given L ; the strength of any additional EUV bump above a simple power-law continuum; variations in the cloud distributions; line and continuum emission anisotropies; variability (the effects of line-continuum lags and the intrinsic Baldwin Effect; Kinney, Rivolo, & Koratkar 1990; Pogge & Peterson 1992). Our aim is to use the more accurate BLR model described here together with the measurements of critical line and continuum strengths to distinguish between as many of these effects as possible and guide us in their empirical calibration. Even a factor of two reduction in the scatter would be an important gain in our ability to use these diagrams for cosmology.

We are grateful for the careful reading and helpful suggestions of the referee, Joe Shields. KTK and GJF acknowledge support from NASA grant NAG-3223 and NSF grant AST 96-17083.

REFERENCES

- Avni, Y., Worrall, D.M., & Morgan, W.A., Jr. 1995, *ApJ*, 454, 673.
- Bahcall, J.N., Kirhakos, S., Saxe, D.H., & Schneider, D.P. 1997, *ApJ*, 479, 642
- Baldwin, J.A. 1977, *ApJ*, 214, 769
- Baldwin, J.A., Wampler, E.J., & Gaskell, C.M. 1989, *ApJ*, 338, 630
- Baldwin, J.A., Ferland, G.J., Korista, K.T., & Verner, D. 1995, *ApJ*, 455, L119
- Baldwin, J.A., Ferland, G.J., Korista, K.T., Carswell, R.F., Hamann, F., Phillips, M.M., Verner, D., Wilkes, B.J., & Williams, R.E. 1996, *ApJ*, 461, 664
- Davidson, K. & Netzer, H. 1979, *Rep. Prog. in Physics* 51, 715
- Espey, B.R., Lanzetta, K.M., & Turnshek, D.A. 1993, *BAAS*, 25, 1448
- Ferland, G.J., Baldwin, J.A., Korista, K.T., Hamann, F., Carswell, R.F., Phillips, M., Wilkes, B., & Williams, R.E. 1996, *ApJ*, 461, 683
- Ferland, G.J., Peterson, B.M., Horne, K.D., Welsh, W.F., & Nahar, S.N. 1992, *ApJ*, 387, 95
- Green, P.J. 1996, *ApJ*, 467, 61
- Green, P.J. 1998, *ApJ*, 498, in press
- Hamann, F., & Ferland, G.J. 1992, *ApJ*, 391, L53
- Hamann, F., & Ferland, G.J. 1993, *ApJ*, 418, 11
- Kinney, A.L., Rivolo, A.R., & Koratkar A.P. 1990, *ApJ*, 357, 338
- Korista, K.T., Baldwin, J.A., & Ferland, G.J. 1997, *ApJS*, 108, 401
- La Franca, F., Franceschini, A., & Vio, R. 1995, *A&A*, 299, 19.
- Laor, A., Bahcall, J.N., Jannuzi, B.T., Schneider, D.P., & Green, R.F. 1995, *ApJS*, 97, 285
- Laor, A., Jannuzi, B.T., Green, R.F., & Boroson, T.A. 1997, *ApJ*, 489, 656
- McLeod, K.K., & Rieke, G.H. 1995a, *ApJ*, 441, 96
- McLeod, K.K., & Rieke, G.H. 1995b, *ApJ*, 454, L77
- Mushotzky, R., & Ferland, G.J. 1984, *ApJ*, 278, 558
- Netzer, H., Laor, Ar., & Gondhalekar, P.M. 1992, *MNRAS*, 254, 15
- Osmer, P.S., Porter, A.C., & Green, R.F. 1994, *ApJ*, 436, 678
- Peterson, B.M. 1993, *PASP*, 105, 247
- Pogge, R.W., & Peterson, B.M. 1992, *AJ*, 103, 1084
- Shields, J.C., Ferland, G.J., & Peterson, B.M. 1995, *ApJ*, 441, 507
- Turnshek, D.A. 1997, in *ASP Conf. Ser. 128, Mass Ejection from AGN*, ed. N. Arav, I. Shlosman, & R.J. Weymann (San Francisco: ASP), 52
- Wang, T.-G., Lu, Y.-J., & Zhou, Y.-Y. 1998, *ApJ*, 493, 1
- Wilkes, B.J., Tananbaum, H., Worrall, D.M., Avni, Y., Oey, M.S., & Flanagan, J. 1994, *ApJS*, 92, 53
- Zamorani, G., et al. 1981, *ApJ*, 245, 357
- Zamorani, G., Marano, B., Mignoli, M., Zitelli, V., & Boyle, B.J. 1992, *MNRAS*, 256, 238
- Zheng, W., Kriss, G.A., & Davidson, A.F. 1995, *ApJ*, 440, 606

This 2-column preprint was prepared with the AAS L^AT_EX macros v4.0.

Fig. 1.— Equivalent widths for full geometric source coverage and intensity ratios from LOC models. (a) W_λ vs. $\log Z$, for $\alpha = 1.4$; (b) $\log W_\lambda$ vs. α , for $\log Z = 0$; (c) \log ratio vs. $\log Z$, for $\alpha = 1.4$; (d) \log ratio vs. α , for $\log Z = 0$.

Fig. 2.— Comparison of LOC results for $Z = 1$ to observed C IV/Ly α (Wang et al. 1998), O VI/Ly α (Zheng et al. 1995).

Fig. 3.— $W_\lambda(\text{C IV})-L_{uv}$ relation calculated for the lowest and highest metallicity Z considered in our models with $\alpha = -1.4$ (solid lines), and for the model in which both Z and the SED are varied together (dashed line), shown overplotted on the observational results of Osmer et al. (1994; data adjusted to $q_o = 0$). Metallicity variations may explain a large part of the observed scatter.

TABLE 1
 ABUNDANCE SETS^a

Z	metals/H	N/H	He/H
0.2	0.2	0.020	0.942
0.5	0.5	0.125	0.964
1	1.0	0.500	1.000
2	2.0	2.000	1.072
5	5.0	12.500	1.290
10	10.0	50.000	1.652

^aRatios X/H relative to solar.

TABLE 2
MODELLED AND OBSERVED CORRELATIONS.

y	x	Slope β		Constant c		Ref ^b	
		Model ^a	Obs ^a	Model ^a	Obs ^a		
$\log W_\lambda(\text{C IV})$	$\log(L_\nu(1550)/10^{30})$	-0.20	-0.25	1.64	1.73	OPG94	
			-0.17		1.92	KRK90	
			-0.23		2.05	L95	
			-0.14			ELT93	
			-0.13			Z92	
			-0.18			T97	
$\log W_\lambda(\text{Ly}\alpha)$	$\log(L_\nu(1550)/10^{30})$	-0.10	-0.13	1.95	2.04	OPG94	
			-0.08		2.12	KRK90	
			-0.14		2.11	L95	
			-0.06			ELT93	
			-0.12			T97	
			-0.30			ZKD95	
$\log W_\lambda(\text{O VI})$	$\log(L_\nu(1550)/10^{30})$			1.60	1.43	L95	
					1.43	ELT93	
						T97	
						ZKD95	
						L95	
						ELT93	
$\log W_\lambda(\text{N V})$	$\log(L_\nu(1550)/10^{30})$			1.43			
					1.47		
						1.12	L95
						1.36	OPG94
							T97
$\log W_\lambda(\text{He II})$	$\log(L_\nu(1550)/10^{30})$			0.828			
					0.863		
						0.77	L95
							T97
							ELT93
							L95
$\log W_\lambda(\lambda 1400)$	$\log(L_\nu(1550)/10^{30})$	-0.13	-0.12	0.985	1.26	L95	
			-0.25			ELT93	
			-0.11			ELT93	
			-0.17			1.52	L95
			-0.05				OPG94
$\log W_\lambda(\lambda 1900)$	$\log(L_\nu(1550)/10^{30})$			1.35			
					1.41		
$\log W_\lambda(\text{Mg II})$	$\log(L_\nu(1550)/10^{30})$	-0.092	-0.05	1.45		ELT93	
			-0.08			Z92	

TABLE 2—*Continued*

y	x	Slope β		Constant c		Ref ^b
		Model ^a	Obs ^a	Model ^a	Obs ^a	
log(Ly α /C IV)	log($L_\nu(1550)/10^{30}$)	0.10	0.12	0.314	0.42	OPG94
			0.09		0.25	KRK90
log(λ 1900/C IV)	log($L_\nu(1550)/10^{30}$)		0.20			OPG94
	log($L_\nu(1550)/10^{30}$) > -0.8	0.12		-0.29		
	log($L_\nu(1550)/10^{30}$) < -0.8	0.20		-0.23		
log(N V/He II)	log(N V/C IV)	0.88	0.90	0.829	0.87	HF93
log(Ly α /C IV)	α_{ox}	0.89		-1.01		
log(Ly α /O VI)	α_{ox}		0.74		-0.38	ZKD95
	$\alpha_{ox} > 1.4$	1.06		-1.04		
	$\alpha_{ox} < 1.4$	0.66		-0.478		

^aColumns 3-6 give results for linear list squares fits to $y = c + \beta x$. The model results assume $q_o = 0$.

^bReferences:

OPG94: Osmer, Porter, & Green (1994). Continuum measured at 1450 Å, $q_o = 0.5$.

KRK90: Kinney, Rivolo, & Koratkar (1990). Continuum measured locally, $q_o = 1$.

L95: Laor et al. (1995). Continuum measured at 1350 Å. Limited (1.5–3 dex) range in L_{uv} , $q_o = 0$.

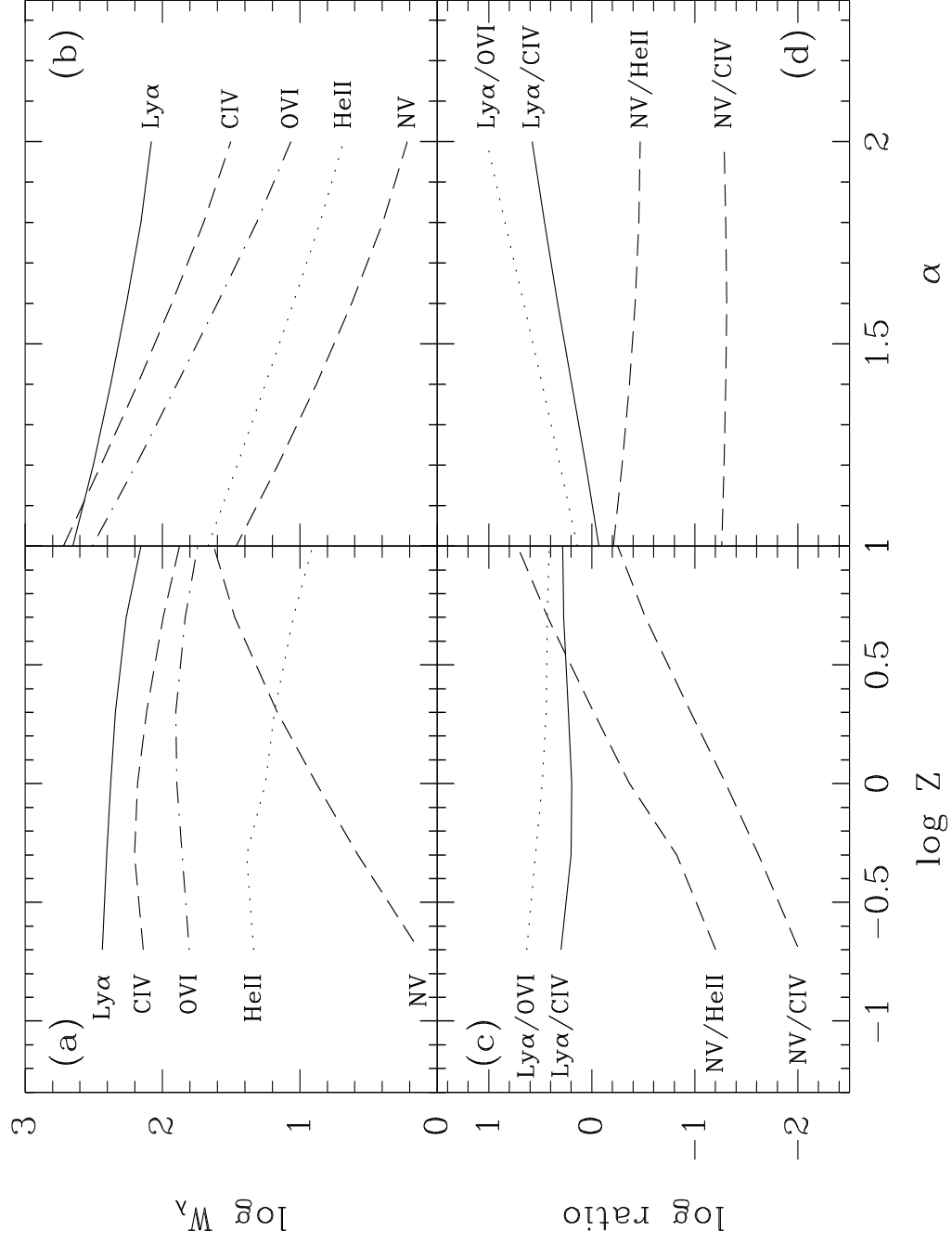
ELT93: Espey, Lanzetta, & Turnshek (1993). Continuum measured at 1450 Å.

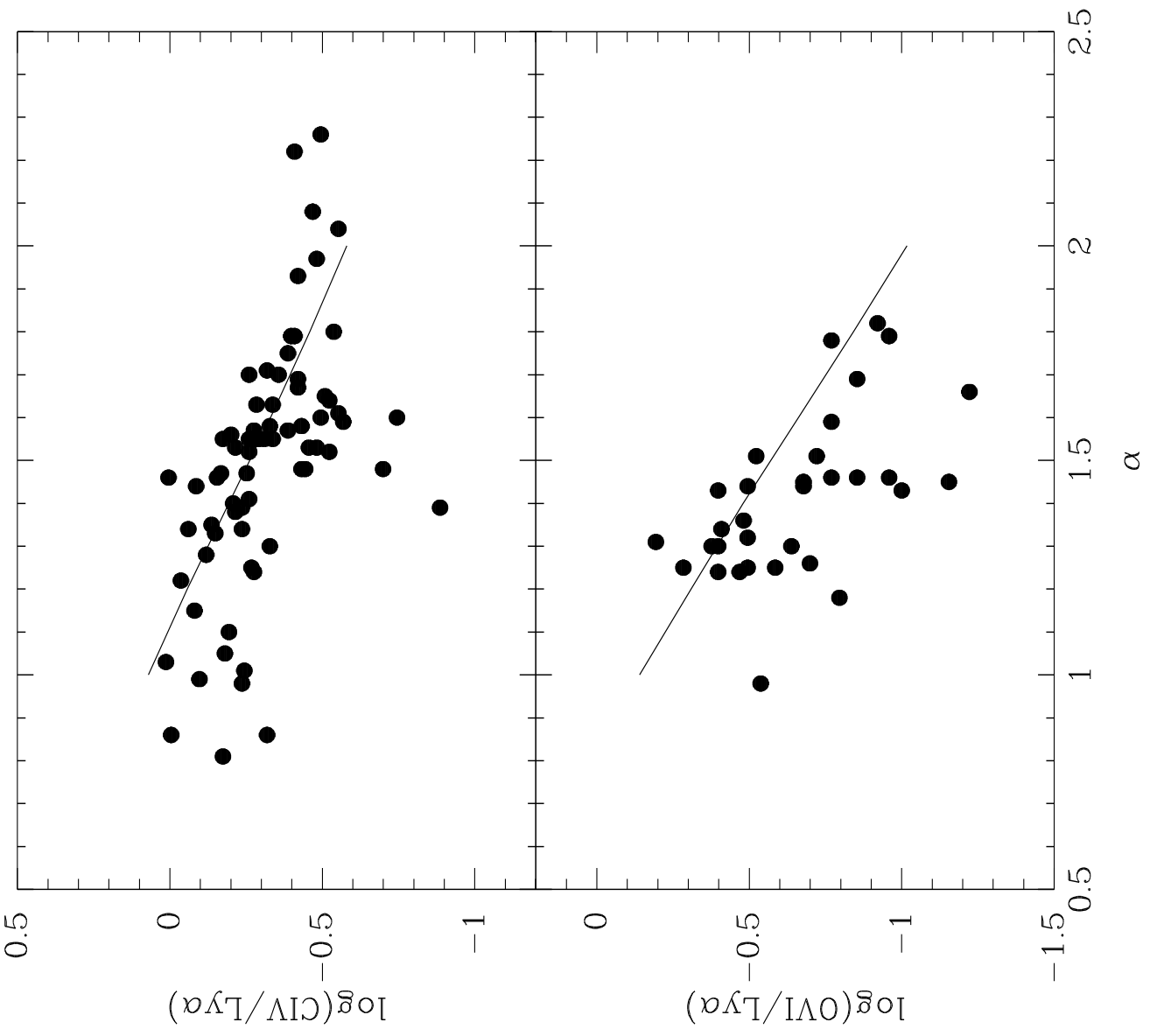
Z92: Zamorani et al. (1992). Limited (2–2.8 dex) range in L_{uv} . Continuum measured locally, $q_o = 1$.

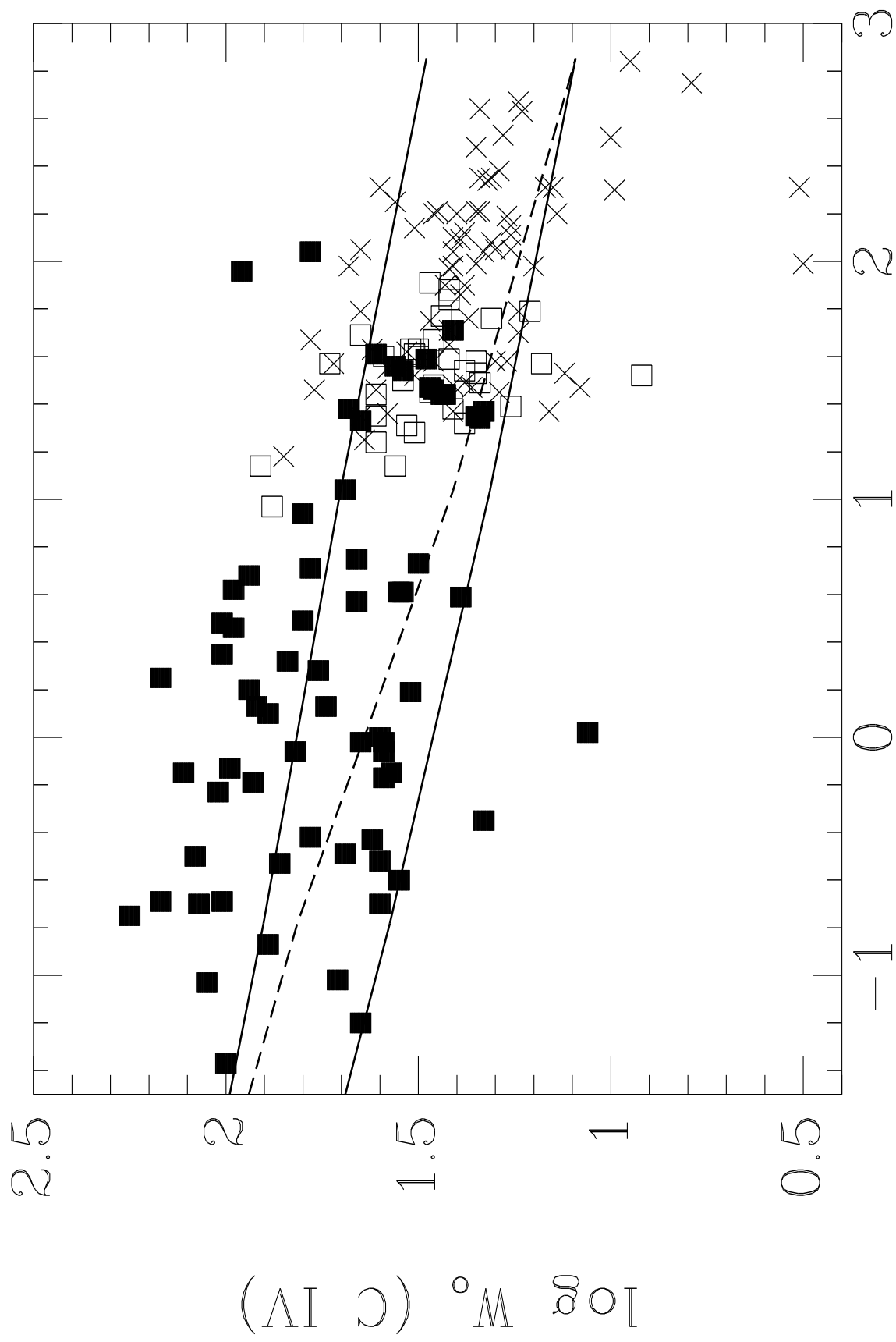
T97: Turnshek (1997).

ZKD95: Zheng, Kriss, & Davidson (1995). Continuum measured at 1550 Å, $q_o = 1$.

HF93: Hamann & Ferland (1993).







$\log L_\nu(1450 \text{ \AA}) - 30$.